JOURNAL OF THERMOPHYSICS AND HEAT TRANSFER
Vol. 9, No. 1, January–March 1995

Refractive Index Effects on Transient Cooling of a Semitransparent Radiating Layer

Robert Siegel*
NASA Lewis Research Center, Cleveland, Ohio 44135

Refractive index effects are examined for transient cooling by radiation and conduction of a gray semitransparent layer. The layer is in a vacuum and so its heat loss is only by internal radiation leaving through its boundaries. Emission within the layer and energy reflected internally from its boundaries increase with the material refractive index. The reflected energy and heat conduction act to distribute energy across the layer and partially equalize the transient temperature distributions. For some conditions significant temperature gradients develop near the boundaries. The numerical solution method provides accurate transient temperature distributions in these regions so that the predicted radiative losses are not in error. An implicit finite difference procedure is used with nonuniform space and time increments. The integrals for the local radiative source in the energy equation are evaluated by Gaussian integration.

Nomenclature

a = absorption coefficient of layer, m^{-1}
c = specific heat of radiating medium, $W \cdot s/kg \cdot K$
D = thickness of radiating layer, m
$E_1, \ldots, E_n$ = exponential integral functions
k = thermal conductivity of layer, $W/m \cdot K$
N = conduction-radiation parameter, $k/4\sigma T_i^3 D$
n = refractive index of layer
q = heat flux, W/m^2
$\tilde{q}$ = dimensionless heat flux $q/\sigma T_i^4$
q_r = radiative heat flow per unit area and time, W/m^2
R = radiation source in energy equation
T = absolute temperature, K
T_e = temperature of surrounding environment, K
T_i = initial temperature of radiating layer, K
T_m = integrated mean temperature, K
t = dimensionless temperature, T/T_i
X = dimensionless coordinate, x/D
x = coordinate in direction across layer, m
ε_m = emittance of layer based on instantaneous value of T_m
ε_{ut} = emittance for a layer at uniform temperature
θ = time, s
κ_D = optical thickness of layer, aD
ρ = density of radiating medium, kg/m^3; reflectivity at a surface
σ = Stefan-Boltzmann constant, $W/m^2 \cdot K^4$
τ = dimensionless time, $(4\sigma T_i^3/\rho c D)\theta$

Subscripts

a, b, c, d = interfaces of layer, Fig. 1
i = initial condition; the ith x location
M = the total number of X grid points
n = at the nth time increment
o = outgoing energy
ut = uniform temperature condition

Introduction

CERAMIC components and coatings are being developed for high-temperature applications in aircraft and automotive engines. The materials are often subjected to transient thermal conditions and may be partially transparent for radiative transfer. Radiative transport within the material acts in combination with heat conduction. The local volume emission within a material depends on the square of its refractive index. Since refractive indices for ceramics are in the approximate range from 1.5 to 3, internal radiation fluxes can be large and are strongly dependent on temperature level. During a transient numerical solution, accurate instantaneous temperature distributions must be obtained or solution inaccuracy will increase as time advances. Two operations are required. The radiative contribution surrounding each location must be integrated to obtain the local absorbed energy within the medium; this was done with Gaussian integration. The transient energy equation must then be solved using this internal energy source that depends on position and time; an implicit finite difference procedure was used with a nonuniform grid. Internal reflections have a large effect on the distribution of absorbed energy. The radiative boundary relations are developed to account for these reflections.

The steady and transient heat transfer behavior of single and multiple plane layer geometries has been examined in the literature for a variety of situations.[1-7] A common boundary condition is to have the absorbing-emitting material contained between walls with specified temperatures. In the present situation the radiating layer is cooled by exposure to a cold environment, and so the layer boundary temperatures are unknown functions of time. The environment is either a vacuum, or external convection is small; hence, there is no means to remove energy from the layer surfaces by external convection or conduction. Since the layer is semitransparent, radiant emission from within its interior passes out through its boundaries. Energy is conducted to the surface, but cannot be radiated exactly from the surface that has no volume. The resulting conduction boundary conditions for the energy equation are a zero-temperature gradient at each surface.

For an optically thick layer the radiative loss through a boundary is mostly from the volume close to the surface. The transient temperature gradient can become large near a boundary, but must go to zero at the boundary. The radiative

Received April 13, 1994; revision received June 28, 1994; accepted for publication June 29, 1994.

*Senior Research Scientist, Research Academy. Fellow AIAA.

loss can be significantly in error if the temperatures near the boundary are inaccurate. The zero temperature gradient boundary condition must be met by the numerical procedure. If not, the solution will behave as if there is an additional energy loss or gain at the boundary; this results in an accumulative error in the overall heat balance during the transient calculations.

In Ref. 5 a finite difference procedure was developed for this type of transient for a material with a refractive index of 1. A nonuniform increment size was used to concentrate grid points near the boundaries. This work is extended here to a layer with a refractive index larger than 1; this requires including effects of internal reflections at the boundaries.

The temperature throughout the layer is initially uniform. As the transient begins, the regions near the boundaries cool rapidly. This reduces the radiative loss since, unless the layer is optically thin, much of the loss is originating from the region where temperature is reduced relative to the layer interior. As cooling continues and the mean temperature decreases, radiation is diminished and the relative effect of conduction increases. Eventually this causes the temperature distribution to become more uniform and emission approaches that of a layer at uniform temperature.

Analysis

Energy Equation for Transient Cooling

A plane layer with thickness D (Fig. 1), is composed of a gray emitting, absorbing, and nonscattering medium that is heat-conducting and has a refractive index larger than 1. The layer is initially at uniform temperature T_i and is then placed in much cooler surroundings so that energy is lost by radiation. The layer is in a vacuum, or external convection is small, so that radiation is the only means for energy loss. The surrounding temperature is low enough that radiation from the surroundings to the layer is neglected.

The transient energy equation is[8]

$$\rho c \frac{\partial T}{\partial \theta} = k \frac{\partial^2 T}{\partial x^2} - \frac{\partial q_r}{\partial x} \tag{1}$$

where the gradient of the radiative flux is given by[8]

$$\frac{\partial q_r}{\partial x} = 4n^2 a\sigma T^4(x, \theta) - 2a\left\{q_{o,b}E_2(ax) + q_{o,c}E_2[a(D - x)] + n^2 a\int_0^D \sigma T^4(x^*, \theta)E_1(a|x^* - x|)\,dx^*\right\} \tag{2}$$

The $q_{o,b}$ and $q_{o,c}$ are the diffuse fluxes in Fig. 1 that are outgoing from the internal boundaries as a result of surface reflections. Thermal properties are assumed independent of temperature.

For convenience, a dimensionless quantity $R(X, \tau)$ is defined as $R(X, \tau) \equiv \frac{1}{4}(\partial \tilde{q}_r/\partial X)$, and so from Eq. (2) in dimensionless form

$$R(X, \tau) \equiv n^2\kappa_D t^4(X, \tau) - \frac{\kappa_D}{2}\left\{\tilde{q}_{o,b}(\tau)E_2(\kappa_D X) + \tilde{q}_{o,c}(\tau)E_2[\kappa_D(1 - X)] + n^2\kappa_D\int_0^1 t^4(X^*, \tau)E_1(\kappa_D|X^* - X|)\,dX^*\right\} \tag{3}$$

The dimensionless energy equation is then

$$\frac{\partial t}{\partial \tau} = N\frac{\partial^2 t}{\partial X^2} - R(X, \tau) \tag{4}$$

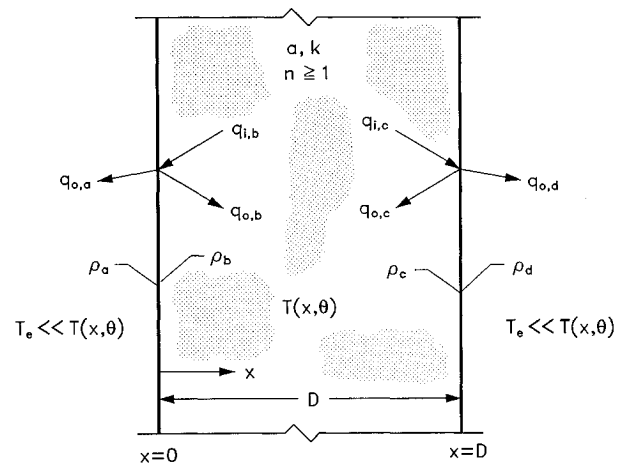

Fig. 1 Geometry, boundary conditions, and nomenclature for plane layer.

Initial and Boundary Conditions

Initially, the layer is at uniform temperature, and so $t(X, 0) = 1$. Boundary conditions must be provided for heat conduction and radiation. Radiation passes out of the layer from within its volume; it is not emitted from the surface itself that has no volume. Then, for a low convection or vacuum environment, no energy is leaving from the planes of the surfaces, and the conduction boundary condition is $\partial t/\partial X = 0$ at $X = 0$ and 1 for all τ.

The radiation boundary conditions are developed in a manner similar to Ref. 9 where steady-state temperatures were obtained for a heated layer with $n > 1$. The boundary conditions provide the fluxes $\tilde{q}_{o,b}$ and $\tilde{q}_{o,c}$ in Eq. (3). Using the interface reflectivities, $\tilde{q}_{o,b} = \rho_b\tilde{q}_{i,b}$ and $\tilde{q}_{o,c} = \rho_c\tilde{q}_{i,c}$ (see Fig. 1). The incident fluxes $\tilde{q}_{i,b}$ and $\tilde{q}_{i,c}$ are obtained from the energy reflected from the opposite boundary and attenuated through the layer, and from energy emission within the layer. These energy quantities are obtained from the radiative flux equation that is the integral of Eq. (2). As detailed in Ref. 9 the $\tilde{q}_{o,b}$ and $\tilde{q}_{o,c}$ are given by

$$\tilde{q}_{o,b}(\tau) = \frac{C_1(\tau) + A_bC_2(\tau)}{1 - A_bA_c} \tag{5a}$$

$$\tilde{q}_{o,c}(\tau) = \frac{C_2(\tau) + A_cC_1(\tau)}{1 - A_bA_c} \tag{5b}$$

where

$$A_b = 2\rho_bE_3(\kappa_D) \tag{5c}$$

$$A_c = 2\rho_cE_3(\kappa_D) \tag{5d}$$

$$C_1(\tau) = 2n^2\rho_b\kappa_D\int_0^1 t^4(X, \tau)E_2(\kappa_D X)\,dX \tag{5e}$$

$$C_2(\tau) = 2n^2\rho_c\kappa_D\int_0^1 t^4(X, \tau)E_2[\kappa_D(1 - X)]\,dX \tag{5f}$$

Although this formulation is general, for the specific computations in this article symmetry gives $A_b = A_c$, $C_1 = C_2$, and $\tilde{q}_{o,b} = \tilde{q}_{o,c}$.

The numerical solution yields transient temperature distributions. Some quantities of interest are the transient mean temperature, the instantaneous heat loss, and the transient emittance of the layer. The instantaneous mean temperature is obtained from

$$T_m(\theta) = \frac{1}{D}\int_0^D T(x, \theta)\,dx \qquad t_m(\tau) = \int_0^1 t(X, \tau)\,dX \tag{6}$$

The instantaneous radiative flux leaving both sides of the layer is equal to $(1 - \rho_b)q_{i,b} + (1 - \rho_c)q_{i,c} = [(1 - \rho_b)/\rho_b]q_{o,b} + [(1 - \rho_c)/\rho_c]q_{o,c}$. Using Eqs. (5a) and (5b), this yields

$$\frac{q_{o,a} + q_{o,d}}{\sigma T_i^4} = \tilde{q}_{o,a} + \tilde{q}_{o,d} = \frac{1 - \rho_b}{\rho_b}\frac{C_1 + A_b C_2}{1 - A_b A_c} + \frac{1 - \rho_c}{\rho_c}\frac{C_2 + A_c C_1}{1 - A_b A_c} \tag{7}$$

To define a transient emittance the instantaneous mean temperature is chosen as a meaningful characteristic temperature. The instantaneous heat dissipation from both sides of the layer is then $2\varepsilon_m(\theta)\sigma T_m^4(\theta)$, so that

$$\varepsilon_m(\tau) = \frac{\tilde{q}_{o,a}(\tau) + \tilde{q}_{o,d}(\tau)}{2t_m^4(\tau)} \tag{8a}$$

To check numerical accuracy the $\varepsilon_m(\tau)$ is obtained by a second method. The local temperature derivative with time is obtained during the numerical solution from the finite difference representation of Eq. (4). Then the emittance is found from the energy balance $2\varepsilon_m(\theta)\sigma T_m^4(\theta) = -\rho c D\, dT_m/d\theta$. This yields

$$\varepsilon_m(\tau) = -\frac{\rho c}{2\sigma T_m^4}\int_0^D \frac{\partial T}{\partial \theta}\,dx = -\frac{2}{t_m^4}\int_0^1 \frac{\partial t}{\partial \tau}\,dX \tag{8b}$$

which is compared with the $\varepsilon_m(\tau)$ from Eq. (8a). Excellent agreement was obtained.

Some useful comparisons can be made by calculating results using the simplifying assumption that the transient temperature distribution remains uniform across the layer. The emittance for this case is called ε_{ut} and is derived in Ref. 10. Interface reflectivities are included to account for internal reflections, and $\rho_b = \rho_c \equiv \rho_{b,c}$ is the same at the inside of both boundaries

$$\varepsilon_{ut} = n^2(1 - \rho_{b,c})\frac{1 - 2E_3(\kappa_D)}{1 - 2\rho_{b,c}E_3(\kappa_D)} \tag{9}$$

For $\varepsilon_m(\tau) = \varepsilon_{ut}$, the integration from $T_m(0) = T_i$ to $T_m(\tau)$ of the heat balance given prior to Eq. (8b) yields

$$T_{ut}(\tau)/T_i = t_{ut}(\tau) = (1 + \tfrac{3}{2}\varepsilon_{ut}\tau)^{-1/3} \tag{10}$$

Then using $q_{ut}(\theta) = \varepsilon_{ut}\sigma T_{ut}^4(\theta)$, the instantaneous energy flux from a layer at uniform, but time varying, temperature is

$$q_{ut}(\tau)/\sigma T_i^4 = \varepsilon_{ut}(1 + \tfrac{3}{2}\varepsilon_{ut}\tau)^{-4/3} \tag{11}$$

Numerical Solution Procedure

To derive a transient solution procedure for Eq. (4), the method in Ref. 5 is further developed to include a refractive index greater than 1. To advance in time, trapezoidal integration over a small $\Delta\tau$ gives the change in t in terms of $\partial t/\partial\tau$ as

$$\Delta t = t_{n+1} - t_n = \int_\tau^{\tau+\Delta\tau}\frac{\partial t}{\partial \tau}\,d\tau \approx \frac{\Delta\tau}{2}\left[\left(\frac{\partial t}{\partial \tau}\right)_{n+1} + \left(\frac{\partial t}{\partial \tau}\right)_n\right] \tag{12}$$

The second derivative at $\tau + \Delta\tau$, that corresponds to the index $n + 1$, is written in terms of Δt and t at τ (index n) by the identity

$$\left(\frac{\partial^2 t}{\partial X^2}\right)_{n+1} + \frac{\partial^2(t_{n+1} - t_n)}{\partial X^2} + \frac{\partial^2 t_n}{\partial X^2} = \frac{\partial^2 \Delta t}{\partial X^2} + \frac{\partial^2 t_n}{\partial X^2} \tag{13}$$

At each X the $R(\tau + \Delta\tau) = R_{n+1}$ is expressed in terms of $R(\tau) = R_n$ by

$$R_{n+1} = R_n + \left(\frac{\partial R}{\partial t}\right)_n (t_{n+1} - t_n) \tag{14}$$

By substituting Eq. (4) into Eq. (12) and using Eqs. (13) and (14), an equation for $\Delta t = t_{n+1} - t_n$ is obtained as

$$\left[1 + \frac{\Delta\tau}{2}\left(\frac{\partial R}{\partial t}\right)_n - \frac{\Delta\tau}{2}N\left.\frac{\partial^2}{\partial X^2}\right|_n\right]\Delta t = \Delta\tau\left[N\left(\frac{\partial^2 t}{\partial X^2}\right)_n - R_n\right] \tag{15}$$

Since all terms in Eq. (15) are at the time corresponding to the index n, this subscript is omitted in what follows. The i subscript is used to specify the X location, where $i = 1$ at $X = 0$, and $i = M$ at $X = 1$. Variable ΔX increment sizes are used across the layer, with ΔX_i^- and ΔX_i^+ extending in the negative and positive directions about each X_i. The second derivative in Eq. (15) is then represented as

$$\left(\frac{\partial^2 t}{\partial X^2}\right)_i = \frac{2t_{i+1}}{\Delta X_i^+(\Delta X_i^+ + \Delta X_i^-)} - \frac{2t_i}{\Delta X_i^+\Delta X_i^-} + \frac{2t_{i-1}}{\Delta X_i^-(\Delta X_i^+ + \Delta X_i^-)} \qquad 1 \le i \le M \tag{16}$$

Relations are now developed for obtaining Δt_i at the grid locations across the layer at time τ_n. This gives the temperatures for all X_i at $\tau + \Delta\tau$ by using $t_{n+1} = t_n + \Delta t_n$ at each X_i. Eq. (16) is substituted into Eq. (15) to give

$$-\frac{\Delta\tau N}{\Delta X_i^-(\Delta X_i^+ + \Delta X_i^-)}\Delta t_{i-1} + \left[1 + \frac{\Delta\tau}{2}\left(\frac{\partial R}{\partial t}\right)_i + \frac{\Delta\tau N}{\Delta X_i^+\Delta X_i^-}\right]\Delta t_i - \frac{\Delta\tau N}{\Delta X_i^+(\Delta X_i^+ + \Delta X_i^-)}\Delta t_{i+1} = \Delta\tau\left\{\frac{2N}{\Delta X_i^+ + \Delta X_i^-}\left[\frac{t_{i+1}}{\Delta X_i^+} - \left(\frac{\Delta X_i^+ + \Delta X_i^-}{\Delta X_i^+\Delta X_i^-}\right)t_i + \frac{t_{i-1}}{\Delta X_i^-}\right] - R_i\right\} \tag{17a}$$

This applies at the interior points $2 \le i \le M - 1$. To account for the zero temperature derivative at each boundary, Eq. (17a) has a special form obtained by letting the temperature at a mirror image grid point be equal to the value at the first grid point away from the boundary. Then for $i = 1$, Eq. (17a) is modified by having the value at the fictitious point $i = 0$ be $t_0 = t_2$, and letting $\Delta X_1^- = \Delta X_1^+$. This gives for $i = 1$, and similarly for $i = M$

$$\left[1 + \frac{\Delta\tau}{2}\left(\frac{\partial R}{\partial t}\right)_1 + \frac{\Delta\tau N}{(\Delta X_1^+)^2}\right]\Delta t_1 - \frac{\Delta\tau N}{(\Delta X_1^+)^2}\Delta t_2 = \Delta\tau\left[\frac{2N}{(\Delta X_1^+)^2}(t_2 - t_1) - R_1\right] \tag{17b}$$

$$-\frac{\Delta\tau N}{(\Delta X_M^-)^2}\Delta t_{M-1} + \left[1 + \frac{\Delta\tau}{2}\left(\frac{\partial R}{\partial t}\right)_M + \frac{\Delta\tau N}{(\Delta X_M^-)^2}\right]\Delta t_M = \Delta\tau\left[\frac{2N}{(\Delta X_M^-)^2}(t_{M-1} - t_M) - R_M\right] \tag{17c}$$

Equations (17a–17c) provide a tridiagonal array for $\Delta t_1 \ldots \Delta t_M$

$$\begin{bmatrix} b_1 & c_1 & & & \\ a_2 & \ddots & \ddots & & \\ & \ddots & \ddots & \ddots & \\ & & \ddots & \ddots & c_{M-1} \\ & & & a_M & b_M \end{bmatrix} \begin{bmatrix} \Delta t_1 \\ \Delta t_2 \\ \vdots \\ \Delta t_{M-1} \\ \Delta t_M \end{bmatrix} = \begin{bmatrix} s_1 \\ s_2 \\ \vdots \\ s_{M-1} \\ s_M \end{bmatrix} \tag{18}$$

where

$$a_i = -\frac{\Delta\tau N}{\Delta X_i^- (\Delta X_i^+ + \Delta X_i^-)} \qquad 2 \le i \le M-1$$

$$a_M = -\frac{\Delta\tau N}{(\Delta X_M^-)^2}$$

$$b_1 = 1 + \frac{\Delta\tau}{2}\left(\frac{\partial R}{\partial t}\right)_1 + \frac{\Delta\tau N}{(\Delta X_1^+)^2}$$

$$b_i = 1 + \frac{\Delta\tau}{2}\left(\frac{\partial R}{\partial t}\right)_i + \frac{\Delta\tau N}{(\Delta X_i^+ \Delta X_i^-)} \qquad 2 \le i \le M-1$$

$$b_M = 1 + \frac{\Delta\tau}{2}\left(\frac{\partial R}{\partial t}\right)_M + \frac{\Delta\tau N}{(\Delta X_M^-)^2}$$

$$c_1 = -\frac{\Delta\tau N}{(\Delta X^+)^2}$$

$$c_i = -\frac{\Delta\tau N}{\Delta X_i^+ (\Delta X_i^+ + \Delta X_i^-)} \qquad 2 \le i \le M-1$$

$$s_1 = \Delta\tau\left[\frac{2N}{(\Delta X_1^+)^2}(t_2 - t_1) - R_1\right]$$

$$s_i = \Delta\tau\left\{\frac{2N}{\Delta X_i^+ + \Delta X_i^-}\left[\frac{t_{i+1}}{\Delta X_i^+} - \left(\frac{\Delta X_i^+ + \Delta X_i^-}{\Delta X_i^+ \Delta X_i^-}\right) t_i + \frac{t_{i-1}}{\Delta X_i^-}\right] - R_i\right\} \qquad 2 \le i \le M-1$$

$$s_M = \Delta\tau\left[\frac{2N}{(\Delta X_M^-)^2}(t_{M-1} - t_M) - R_M\right]$$

The $\partial R/\partial t$ is needed at each X_i for the b_i coefficients. Using $R(X, \tau)$ in Eq. (3), $\partial R/\partial t|_X = (\partial R/\partial\tau|_X)/(\partial t/\partial\tau|_X)$, which gives

$$\left.\frac{\partial R}{\partial t}\right|_X = 4n^2\kappa_D t^3(X, \tau) - \frac{\frac{\kappa_D}{2}\left\{\left(\frac{d\tilde{q}_{o,b}(\tau)}{d\tau}E_2(\kappa_D X) + \frac{d\tilde{q}_{o,c}(\tau)}{d\tau}E_2[\kappa_D(1-X)]\right) + 4n^2\kappa_D\int_0^1 t^3(X^*, \tau)\left.\frac{\partial t(X^*, \tau)}{\partial\tau}\right|_{X^*} E_1(\kappa_D|X^* - X|)\,dX^*\right\}}{\left.\frac{\partial t(X, \tau)}{\partial\tau}\right|_X} \tag{19}$$

The $\partial t(X, \tau)/\partial\tau$ is obtained during the solution from the finite difference representation of Eq. (4). The derivatives of $\tilde{q}_{o,b}$ and $\tilde{q}_{o,c}$ in Eq. (19) are evaluated from relations in Eq. (5). This gives

$$\frac{d\tilde{q}_{o,b}(\tau)}{d\tau} = \frac{\frac{dC_1(\tau)}{d\tau} + A_b\frac{dC_2(\tau)}{d\tau}}{1 - A_bA_c}$$

$$\frac{d\tilde{q}_{o,c}(\tau)}{d\tau} = \frac{\frac{dC_2(\tau)}{d\tau} + A_c\frac{dC_1(\tau)}{d\tau}}{1 - A_bA_c} \tag{20}$$

where

$$\frac{dC_1(\tau)}{d\tau} = 8n^2\rho_b\kappa_D\int_0^1 t^3(X, \tau)\left.\frac{\partial t(X, \tau)}{\partial\tau}\right|_X E_2(\kappa_D X)\,dX$$

$$\frac{dC_2(\tau)}{d\tau} = 8n^2\rho_c\kappa_D\int_0^1 t^3(X, \tau)\left.\frac{\partial t(X, \tau)}{\partial\tau}\right|_X E_2[\kappa_D(1-X)]\,dX$$

The tridiagonal array in Eq. (18) is solved using the well-known algorithm.[11,12] The Δt_i at each X_i is added to each t_i value to advance to the next time increment.

To evaluate $R(X)$ and $\partial R/\partial t|_X$ in the matrix coefficients requires an accurate integration method. Since $E_1(0) = \infty$, special treatment is needed as X^* approaches X. The integral of E_1 is $-E_2$, and $E_2(0) = 1$, and so the integration is evaluated analytically for a very small region near the singularity with t^3 or t^4 equal to its value at X. This is shown in Ref. 4 to provide accurate results. Gaussian integration is used for the integrations away from the singularity. Values of the functions at the unevenly spaced points in the Gaussian subroutine were obtained from the grid point values by cubic spline interpolation. By trying various numbers of grid points it was found that 50 ΔX increments across the layer gave accurate results. The increment size was small adjacent to each boundary where 10 increments with $\Delta X = 0.01$ were used. A variable time increment was used with the $\Delta\tau = 0.005$ or 0.0025 initially, and then gradually increased during the calculation as the rate of temperature change decreased.

Results and Discussion

Transient Temperature Distributions

The solution yields transient temperatures starting from an initially uniform temperature. Typical temperature distributions are in Figs. 2a–2c for optical thicknesses $\kappa_D = 2$, 5, and 20. These results are for the limit of zero heat conduction $N = 0$, and so they show the maximum influence of radiation during transient cooling. From symmetry, only half of the layer is shown. Each part of Fig. 2 gives temperature profiles at three dimensionless times during the transient. For each time the three temperature distributions show the effect of refractive index for $n = 1$, 1.5, and 2. The horizontal dot-dash line at each time is computed from Eq. (10). It is the temperature obtained by assuming the temperature profile remains uniform with X, but is a function of time throughout the transient. The ε_{wt} used in Eq. (10) for a layer at uniform temperature is a function of refractive index and optical thickness as given by Eq. (9) and Table 1. The $\rho_{b,c}$ in Eq. (9) is a function of n given by the Fresnel relations in Ref. 9; the dot-dash lines in Fig. 2 are for $n = 1.5$.

The layer is initially at uniform temperature T_i. When the transient begins, the layer is subjected to cold surroundings ($T_c \ll T_i$) and the outer portions cool more rapidly than the interior. For a small optical thickness as in Fig. 2a, the transient temperature profiles are fairly uniform and the results using the uniform temperature assumption provide an approximation for the transient temperature level. When the optical thickness is large as in Fig. 2c, the profiles have a large variation across the layer, and with $N = 0$ the temperatures near each boundary change rapidly with X.

Table 1 Emittance values for a layer at uniform temperature, $\varepsilon_{ut}(n, \kappa_D)$

n	$\kappa_D = 1$	$\kappa_D = 2$	$\kappa_D = 5$	$\kappa_D = 10$	$\kappa_D = 20$
1	0.7806	0.9397	0.9982	1.0000	1.0000
1.5	0.8157	0.8853	0.9076	0.9082	0.9082
2	0.7927	0.8283	0.8391	0.8394	0.8394
2.5	0.7518	0.7720	0.7780	0.7781	0.7781
3	0.7078	0.7201	0.7237	0.7238	0.7238

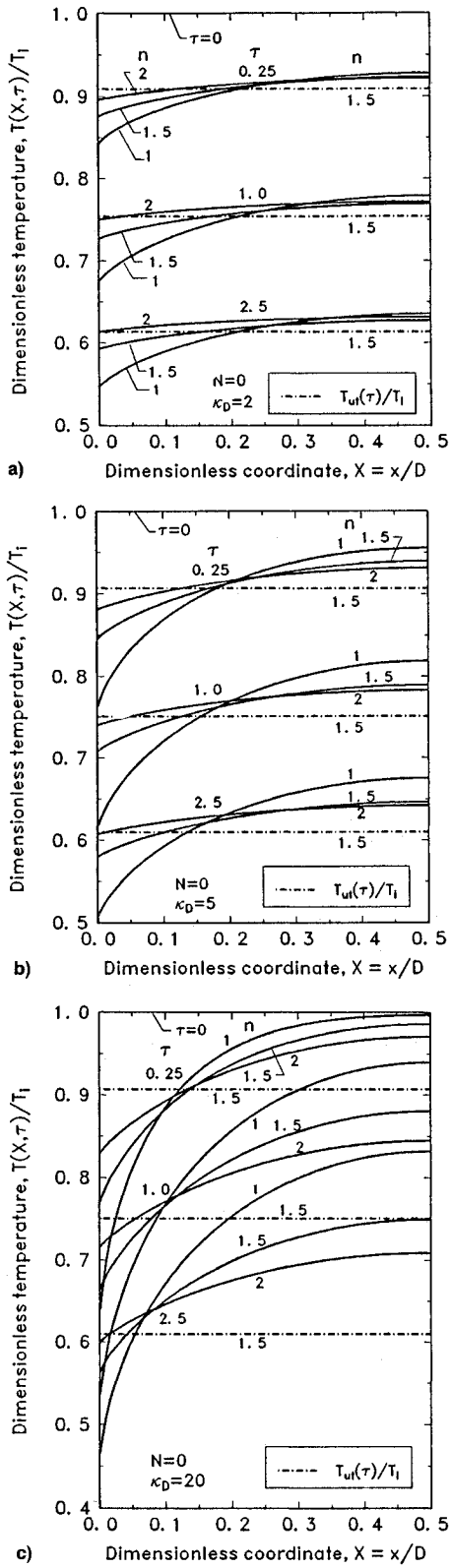

Fig. 2 Effect of refractive index on transient temperature distributions in a layer for three optical thicknesses in the limit of zero heat conduction $N = 0$. K_D = a) 2, b) 5, and c) 20.

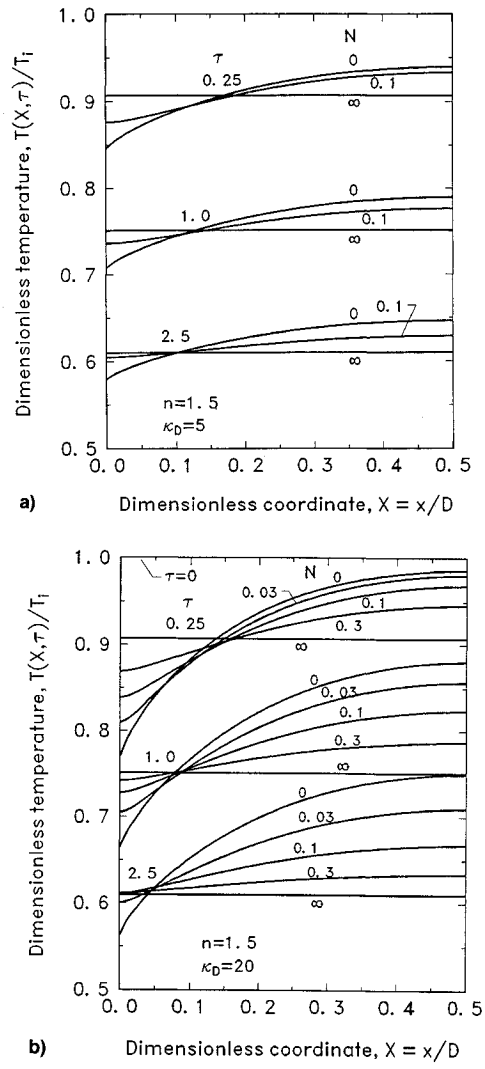

Fig. 3 Effect of conduction-radiation parameter on transient temperature distributions for a layer with refractive index $n = 1.5$ and two optical thicknesses. K_D = a) 5 and b) 20.

The effect of refractive index is to make the profiles more uniform as n is increased. By comparing results for $n = 1$ and 2 it is evident that the refractive index can reduce the amplitude of the temperature variation by a factor of 3 or 4. This is attributed to internal reflections from the boundaries that tend to distribute energy across the layer.

The effect of heat conduction on the temperature profiles is shown in Fig. 3 for $n = 1.5$. When there is heat conduction ($N > 0$), the conditions of the present problem impose a zero temperature gradient at each boundary. In Fig. 3a for $\kappa_D = 5$, a value of $N = 0.1$ provides enough heat conduction to significantly reduce the temperature gradient in the region near the boundary, and the amplitude of the temperature distribution is reduced about in half. Results for additional N values are in Fig. 3b for a larger optical thickness, $\kappa_D = 20$. Except for very near the beginning of the transient, the profiles become rather uniform for N greater than about 0.3.

Transient Mean Temperature

The transient mean temperature of the layer is in Fig. 4a for zero conduction ($N = 0$), which shows the maximum radiative effect during transient cooling. Results are for three optical thicknesses and various refractive indices. The lowest curve (labeled optimum) has the maximum possible cooling rate; it is for a black layer that is always at uniform temperature. When $\kappa_D = 2$ the temperature profiles in Fig. 2a are somewhat uniform. The cooling curve for $n = 1$ in Fig. 4a is above the optimum behavior because the layer is not thick enough to act as a black layer. When n is increased there are two effects. The external reflectivity of the boundaries is increased that decreases the layer absorptance and, hence, its emittance. The temperatures are also raised near the boundaries as the temperature profiles become more uniform; this increases emission. Since the profiles for $\kappa_D = 2$ are already rather uniform, the first effect is dominating and there is a decrease in cooling rate when n is increased from 1 to 2. For $\kappa_D = 20$ (solid lines on Fig. 4a) the low temperatures near the boundaries relative to the much higher interior temperatures during the transient (see Fig. 2c) reduce the cooling effectiveness, and cooling is much slower than for the optimum case of a black layer at uniform temperature. Increasing the refractive index increases the cooling rate by making the temperature profiles more uniform. The effect of n is opposite to that for $\kappa_D = 2$.

For the results in Fig. 4b there is heat conduction with $N = 0.1$. Compared with $N = 0$, the temperature profiles for $N = 0.1$ are more uniform as in Fig. 3. Transient cooling is enhanced as a result of increased temperatures near the boundaries, and the curves in Fig. 4b move closer to the optimum results. For these particular conditions the effect of n decreases with increasing κ_D, which is opposite to the behavior in Fig. 4a. When $\kappa_D = 20$, there is very little effect of refractive index.

A way to present the transient variation in mean temperature in more detail to provide quantitative information is by forming a ratio of transient values with results when the temperature remains spatially uniform throughout the transient [$T(\tau)$ independent of X]. This is the ratio $T_m(\tau)/T_{ut}(\tau)$ of values from Fig. 4a or 4b to those from Eq. (10). For conditions where this ratio is close to one, Eq. (10) can be used to calculate approximate transient mean temperatures. For other conditions the ratio can be used in conjunction with Eq. (10) to obtain accurate estimates of $T_m(\tau)$. Since the ratio extends over a moderate range, values can be interpolated for other values of the parameters. Results for $\kappa_D = 20$ are in Fig. 5. The ordinate is 1.0 for $N \to \infty$; for any finite N the $T_m(\tau)$ is always larger than $T_{ut}(\tau)$. For a small optical thickness the layer temperature distribution remains fairly uniform throughout the transient. As a result, for $\kappa_D = 5$, a figure similar to Fig. 5 shows that $T_m(\tau)$ is a few percent above $T_{ut}(\tau)$, unless n is less than 1.5 and N is less than 0.1. Hence, for $\kappa_D < 5$, Eq. (10) can be used in many instances to obtain an approximation for the instantaneous mean temperature. Similar results for $\kappa_D = 10$ show that for $N > 0.1$ agreement with Eq. (10) is within 5% for all n. For $\kappa_D = 20$ in Fig. 5, the temperature ratio is close to one (within about 3%) for $N > 0.3$.

Transient Heat Loss

The instantaneous heat flux leaving the layer is in Fig. 6 for the same parameters as in Fig. 4. The uppermost curves in Figs. 6a and 6b are for the optimum case of cooling a black layer at uniform temperature throughout the transient. As discussed for Fig. 4a, increasing n in Fig. 6a increases the cooling rate when κ_D is large, but has the opposite effect when κ_D is small. The smallest transient emission is for an optically thick layer with $n = 1$, since the temperatures are decreased near the boundaries as a result of transient cooling. In Fig. 6b, for $N = 0.1$, the curves shift toward the optimum curve as heat conduction makes the temperature profiles more uniform. There is very little effect of refractive index for $\kappa_D = 10$ and 20.

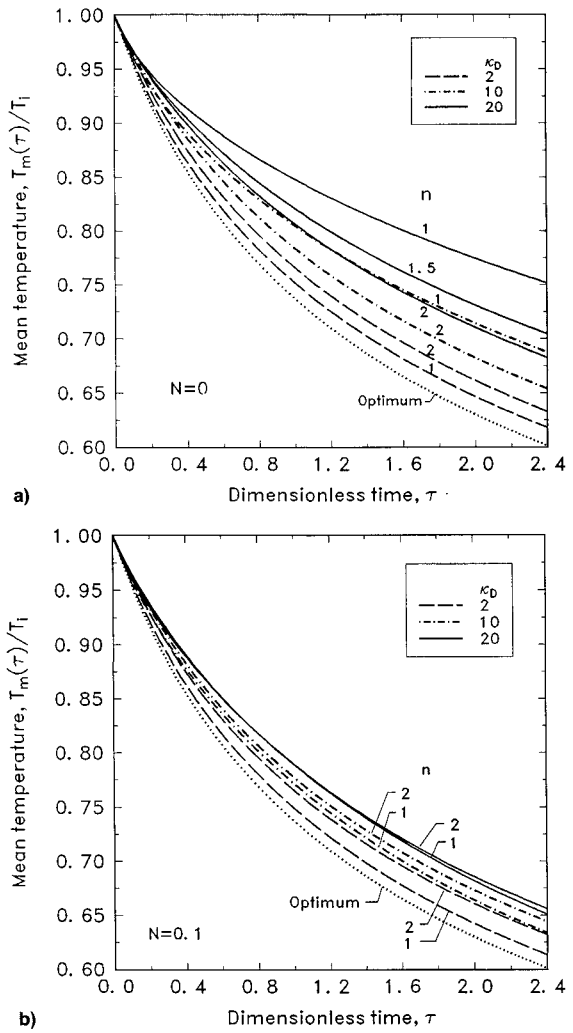

Fig. 4 Effect of refractive index and optical thickness on the transient mean temperature of a layer during cooling: a) zero heat conduction, $N = 0$ and b) conduction-radiation parameter, $N = 0.1$.

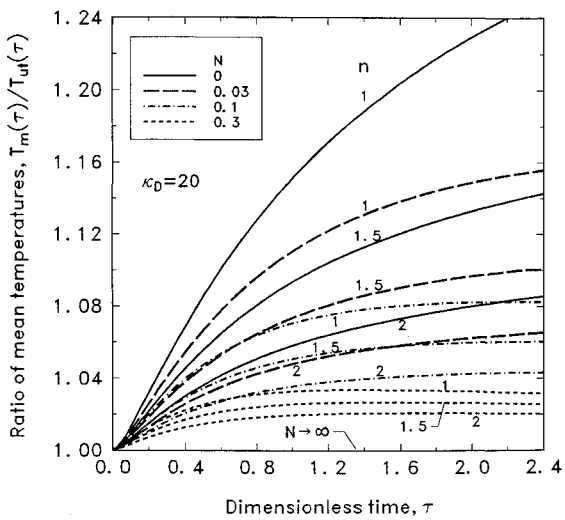

Fig. 5 Mean temperature of a layer during transient cooling compared with that for a layer cooling with a uniform instantaneous temperature distribution; effect of refractive index and heat conduction for $\kappa_D = 20$.

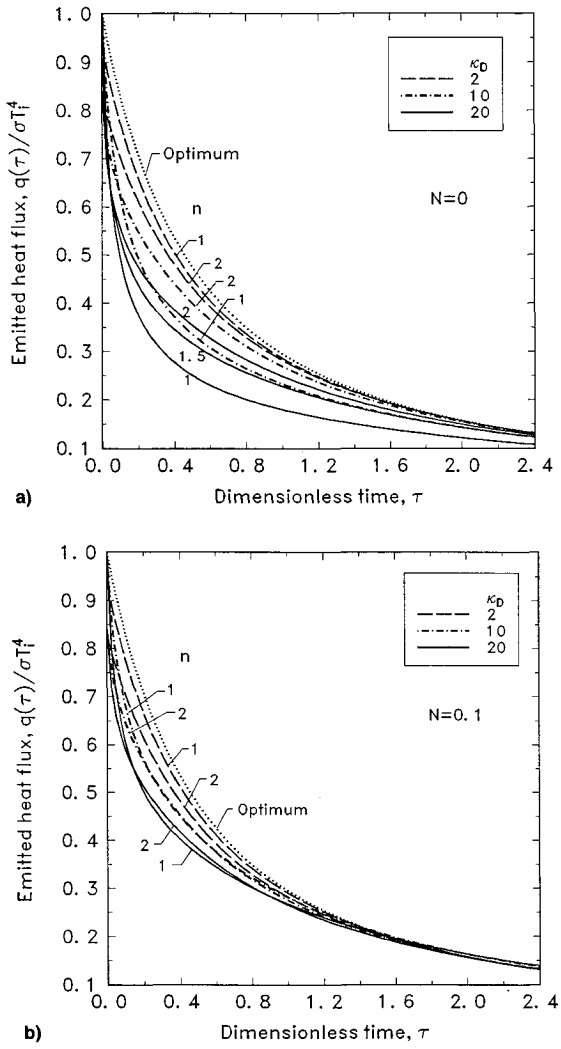

Fig. 6 Effect of refractive index and optical thickness on the transient heat loss from a layer during cooling: a) zero heat conduction, N = 0 and b) conduction-radiation parameter, N = 0.1.

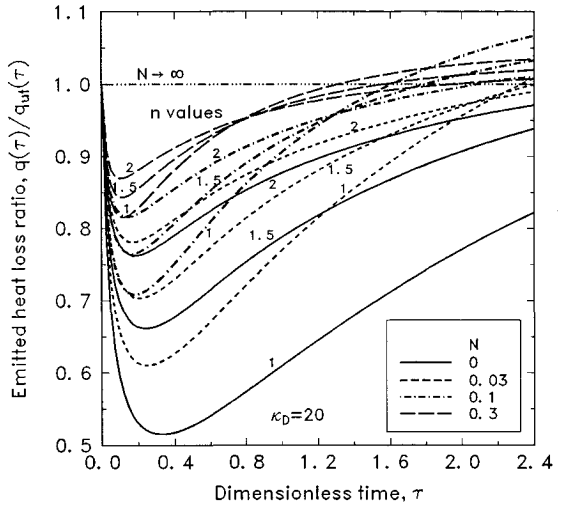

Fig. 7 Heat loss from layer during transient cooling as compared with that for a layer cooling with a uniform instantaneous temperature distribution; effect of refractive index and heat conduction for κ_D = 20.

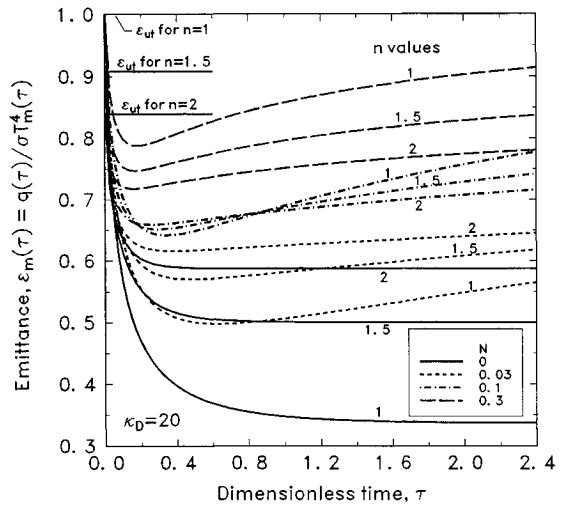

Fig. 8 Transient emittance of a layer during cooling; effect of refractive index and heat conduction for κ_D = 20.

The ordinate in Fig. 7 is the instantaneous heat loss from the layer given as a ratio to the values for a spatially uniform, but time varying, temperature as obtained from Eq. (11); these results are for κ_D = 20. Since values from Eq. (11) are easily calculated, the $q(\tau)$ can be readily obtained from the ratios given and can be interpolated for other parameters. During the early portion of the transient the rate of energy loss is lower than for a layer with $T(\tau)$ independent of X. As time proceeds some of the ratios become a little larger than 1. This is because the mean temperature has decreased more slowly than for the uniform temperature case. Late in the transient the mean temperature is large enough that the heat loss exceeds that reached for the spatially uniform temperature layer at that time.

Transient Emittance

The transient emittance is the instantaneous heat flux radiated from one side of the layer divided by $\sigma T_m^4(\tau)$. It is calculated from values as in Figs. 4 and 6. Results for κ_D = 20 and various n and N are in Fig. 8. Since the layer temperature is initially uniform, the emittance at τ = 0 is ε_{ut} in Table 1 or Eq. (9). The curves in Fig. 8 begin at these values. For $N \rightarrow \infty$, conduction equalizes the temperature distribution so that the emittance remains at ε_{ut} throughout the transient; for N = 0 there is radiation only. As the transient begins, the temperatures decrease near the boundary and the emittance decreases rapidly since the radiation loss is smaller than that characteristic of the layer instantaneous mean temperature. As shown by the similarity solution in Ref. 7, for n = 1 and N = 0, the transient emittance decreases to a steady value that depends on the layer optical thickness; the present results show that this behavior remains valid for $n > 1$. With conduction present ($N > 0$), the temperature distribution gradually becomes more uniform as the transient proceeds; and as temperatures decrease, radiation becomes less important and conduction begins to dominate. The transient emittance then rises toward its initial value corresponding to a uniform temperature layer.

Concluding Remarks

Transient solutions were obtained for a radiating and conducting layer cooled by exposure to a cold vacuum environment. The layer has diffuse surfaces and a refractive index larger than 1. A transient finite difference solution procedure is used; computer times on a Cray X-MP are 2–3 min for a complete transient solution. Transient mean temperatures and heat losses were compared with analytical results for a layer at uniform temperature at any instant during the transient, and with the optimum case of a black layer at uniform, but time-varying, temperature. There are two effects of refractive index. One is that internal reflections help distribute energy

within the layer, which tends to make the transient distributions more uniform. This increases emission by preventing low temperatures near the boundaries. However, reflections from the boundaries also tend to contain radiation within the layer that reduces cooling for a larger n. For optically thin layers where the temperature distribution is already rather uniform, the second effect dominates, and increasing n can decrease the cooling rate. For larger optical thicknesses the first effect is more important, and so increasing n augments cooling by helping to prevent the transient temperatures from becoming low near the boundaries.

References

[1]Tsai, C.-F., and Nixon, G., "Transient Temperature Distribution of a Multilayer Composite Wall with Effects of Internal Thermal Radiation and Conduction," *Numerical Heat Transfer*, Vol. 10, No. 1, 1986, pp. 95–101.

[2]Tarshis, L. A., O'Hara, S., and Viskanta, R., "Heat Transfer by Simultaneous Conduction and Radiation for Two Absorbing Media in Intimate Contact," *International Journal of Heat and Mass Transfer*, Vol. 12, No. 3, 1969, pp. 333–347.

[3]Viskanta, R., and Grosh, R. J., "Heat Transfer by Simultaneous Conduction and Radiation in an Absorbing Medium," *Journal of Heat Transfer*, Vol. 84, No. 1, 1962, pp. 63–72.

[4]Siegel, R., "Transient Radiative Cooling of a Droplet-Filled Layer," *Journal of Heat Transfer*, Vol. 109, No. 1, 1987, pp. 159–164.

[5]Siegel, R., "Finite Difference Solution for Transient Cooling of a Radiating-Conducting Semitransparent Layer," *Journal of Thermophysics and Heat Transfer*, Vol. 6, No. 1, 1992, pp. 77–83.

[6]Baek, S. W., Kim, T. Y., and Lee, J. S., "Transient Cooling of a Finite Cylindrical Medium in the Rarefied Cold Environment," *International Journal of Heat and Mass Transfer*, Vol. 36, No. 16, 1993, pp. 3949–3956.

[7]Siegel, R., "Separation of Variables Solution for Non-Linear Radiative Cooling," *International Journal of Heat and Mass Transfer*, Vol. 30, No. 5, 1987, pp. 959–965.

[8]Siegel, R., and Howell, J. R., *Thermal Radiation Heat Transfer*, 3rd ed., Hemisphere, Washington, DC, 1992.

[9]Spuckler, C. M., and Siegel, R., "Refractive Index Effects on Radiative Behavior of a Heated Absorbing-Emitting Layer," *Journal of Thermophysics and Heat Transfer*, Vol. 6, No. 4, 1992, pp. 596–604.

[10]Siegel, R., and Spuckler, C. M., "Effects of Refractive Index and Diffuse or Specular Boundaries on a Radiating Isothermal Layer," *Journal of Heat Transfer*, Vol. 116, No. 3, 1994, pp. 787–790.

[11]Varga, R. S., *Matrix Iterative Analysis*, Prentice-Hall, Englewood Cliffs, NJ, 1962.

[12]Press, W. H., Flannery, B. P., Teukolsky, S. A., and Vetterling, W. T., *Numerical Recipes*, Cambridge Univ. Press, New York, 1989.